

# Strain-space model for Sars-CoV-2

Peter C. Jentsch, PhD <sup>1,4</sup>    Finlay Maguire, PhD <sup>3,5</sup>  
Samira Mubareka, MD, FRCPC <sup>1,2</sup>

<sup>1</sup>Sunnybrook Research Institute, Toronto, Canada

<sup>2</sup>University of Toronto, Toronto, Canada

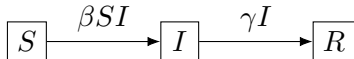
<sup>3</sup>Dalhousie University, Halifax, Canada

<sup>4</sup>Simon Fraser University, Burnaby, Canada

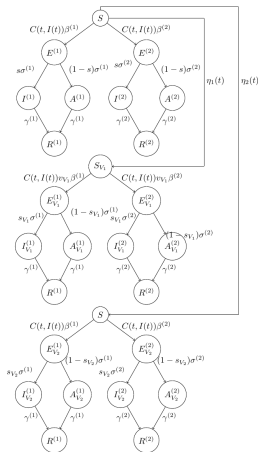
<sup>5</sup>Shared Hospital Laboratory, Toronto, Canada

June 29, 2022

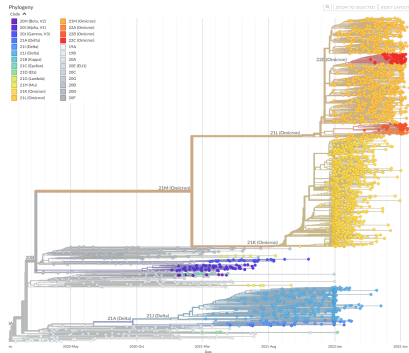
- Infection spread is often modelled using compartmental models
- Represent subsets of a host population and rates of movement between them



- Multiple infections (e.g. competing VoCs) can be represented as more compartments
- Work on multiple infections is usually here due to lack of data, increasing complexity

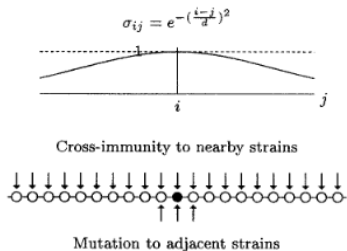


This only represents a tiny amount of the genomic data we have for Sars-CoV-2!

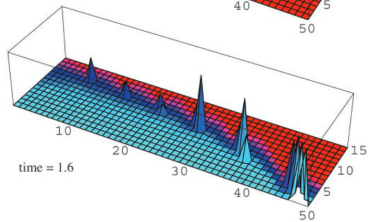
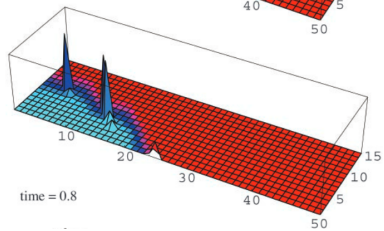
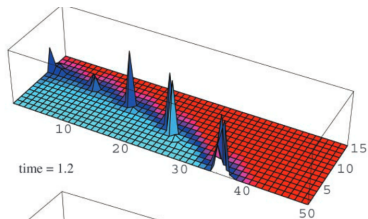
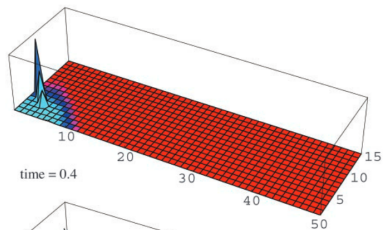


- Can extend these models to a sequence of variants
- Assume each variant is indexed by  $i$
- The dynamics at each variant  $i$  are determined by a simple compartmental model

- Variants are related by a function  $\sigma(i, j)$  that determines how much an infection by variant  $i$  reduces probability of infection to variant  $j$ .
- A variant  $i$  mutates to neighbouring indices  $i + 1, i - 1$  proportional to the population of variant  $i$



[Gog and Grenfell, 2002]

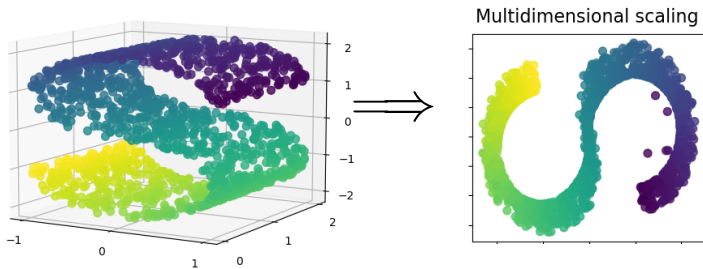


[Gog and Grenfell, 2002]

# Antigenic cartography

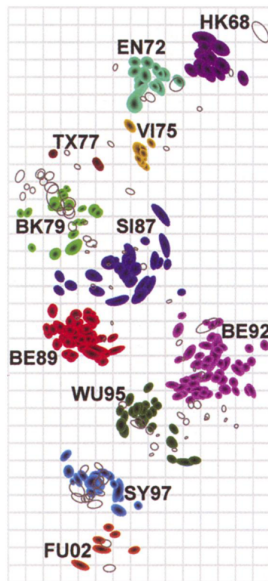
- Practice of mapping out immune responses to related pathogens
- Distance between serums and pathogen is quantified, these points are visualized using multidimensional scaling



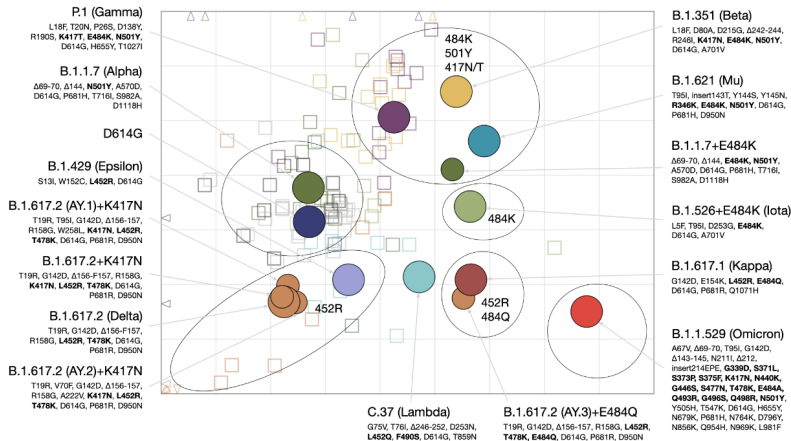


[Pedregosa et al., 2011]

This technique was developed to visualize the antigenic drift of H3N2



[Lapedes and Farber, 2001, Smith et al., 2004]



[Wilks et al., 2022]

These results suggest that 2 dimensions might be an adequate approximation to the full space!

# Model Equations

$$\frac{S_{ij}}{dt} = - \sum_{kl} \beta_{kl} \sigma_{ijkl} S_{ij} I_{kl} + \gamma R_{ij} \quad (1)$$

$$\frac{I_{ij}(t)}{dt} = \beta_{ij} S_{ij} I_{ij} - \xi I_{ij} + M (-4I_{ij} + I_{i-1,j} + I_{i+1,j} + I_{i,j-1} + I_{i,j+1}) \quad (2)$$

$$\frac{R_{ij}(t)}{dt} = \xi I_{ij} - \gamma R_{ij} \quad (3)$$

Boundary conditions:  $I_{0,j} = 0, I_{j,0} = 0, I_{N,j} = 0, I_{j,N} = 0$   
Initial conditions computed from genomic data in GISAID

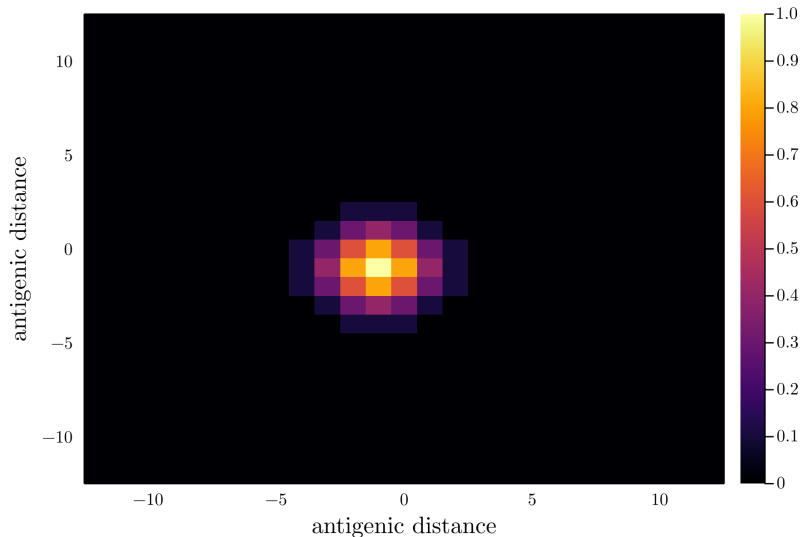
## Model parameters/variables

Symbol	Description
$N$	Size of variant grid
$S_{ij}$	Population susceptible to variant $(i, j) \in [0, N]^2$
$I_{ij}$	Population infected by variant $(i, j) \in [0, N]^2$
$R_{ij}$	Recovered/Immune to variant $(i, j) \in [0, N]^2$
$\sigma_{ijkl}$	Probability that exposure to variant $(i, j)$ causes immunity to variant $(k, l)$
$\beta_{ij}$	Transmission rate of variant $(i, j)$
$\xi$	Recovery rate of all strains
$\gamma$	Rate of immunity loss of all strains

Table of symbols for Model 2

## $\sigma$ matrix

In practice, we assume  $\sigma_{ijkl}$  is just a 2-D gaussian distribution parameterized by the distance between  $(i, j)$  and  $(k, l)$ .



To incorporate more realistic mutation rates, we can go to continuous strain-space and use nonlocal reaction-diffusion dynamics as in [Rouzine and Rozhnova, 2018, Bessonov et al., 2021]

$$S_t(x, y, t) = \int_{-\infty}^{\infty} \int_{-\infty}^{\infty} \beta(x', y') \sigma(x, y, x', y') S(x, y, t) I(x', y', t) dx' dy' + \gamma R_{ij} - \eta(t) v(x, y) S(x, y, t) \quad (4)$$

$$I_t(x, y, t) = \beta(x, y) S(x, y, t) I(x, y, t) - \xi I(x, y, t) + M (I_x(x, y, t) + I_y(x, y, t)) \quad (5)$$

$$R_t(x, y, t) = \xi I(x, y, t) I(x, y, t) - \gamma R(x, y, t) + \eta(t) v(x, y) S(x, y, t) \quad (6)$$

where  $\beta, \sigma, v$  have been generalized to their continuous counterparts. Given a dispersion kernel  $K(x, y) \in L_2 : \mathbb{R}^2 \rightarrow \mathbb{R}$  this can be generalised to non-local diffusion as follows

$$I_t(x, y, t) = \beta(x, y) S(x, y, t) I(x, y, t) - \xi I(x, y, t) + M \left( \int_{-\infty}^{\infty} \int_{-\infty}^{\infty} K(x - x', y - y') I(x', y', t) dx' dy' \right) \quad (7)$$



# Developing an antigenic distance map

- We would like an approximate measure of antigenic distance for every sample genome
- Using all samples, we compute pairwise distances between each unique genome in some way that encodes antigenic response
- Many possible ways to do this, so far none of them seem to work very well
- Project to 2-d (hopefully) space with multidimensional scaling

# Genome distance

Assume:

- $a, b$  are SARS-CoV-2 genomes aligned with the reference
- $a_i$  the  $i$ th nucleotide base in  $a$  and

$$\chi(a_i, b_i) = \begin{cases} 1 & \text{if } a_i = b_i \\ 0 & \text{otherwise} \end{cases}$$

- $h_i$  is a vector containing the number of homoplasic mutations at site  $i$  in the global tree
- $\mathfrak{B}(a)$  computes the polyclonal binding affinity of genome  $a$  as per [Starr et al., 2020]

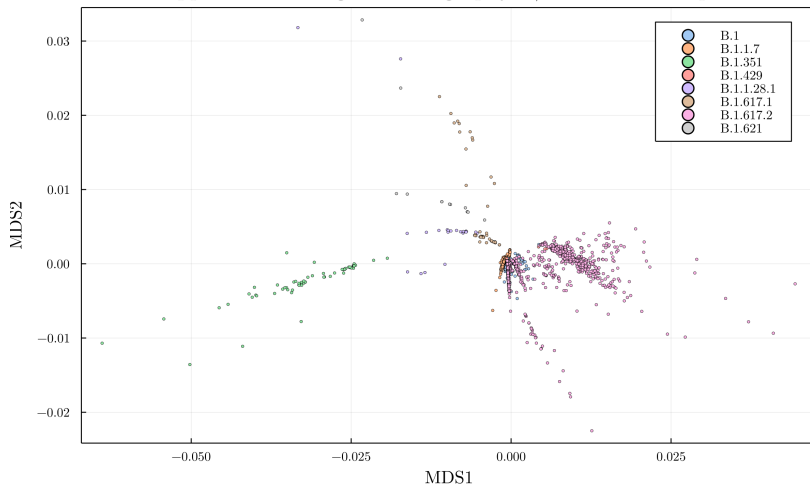
One option for a distance measure is something like

$$d(a, b) = \frac{\mathfrak{B}(a) + \mathfrak{B}(b)}{2} + \sum_i \chi(a_i, b_i) h_i \quad (8)$$

That is, the average binding between two genomes plus the SNP distance weighted by the relative homoplasmy of each mutation.

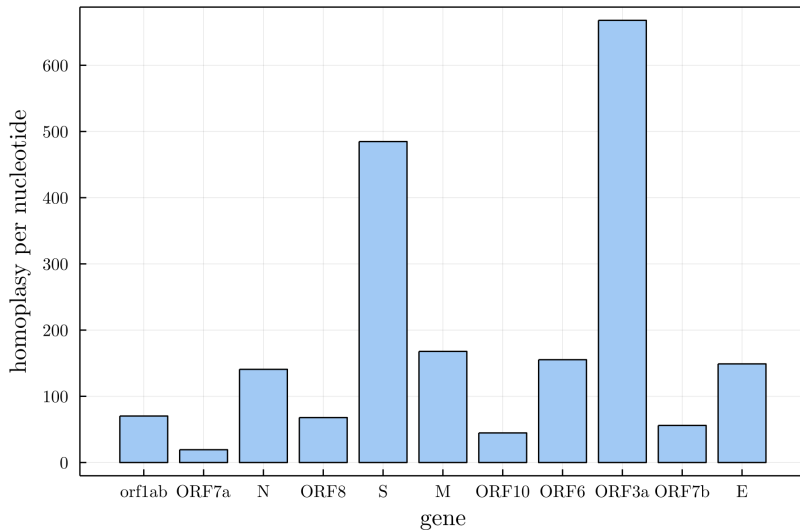
# Example antigenic distance map

Approximate antigenic cartography w/ RBD, UK samples



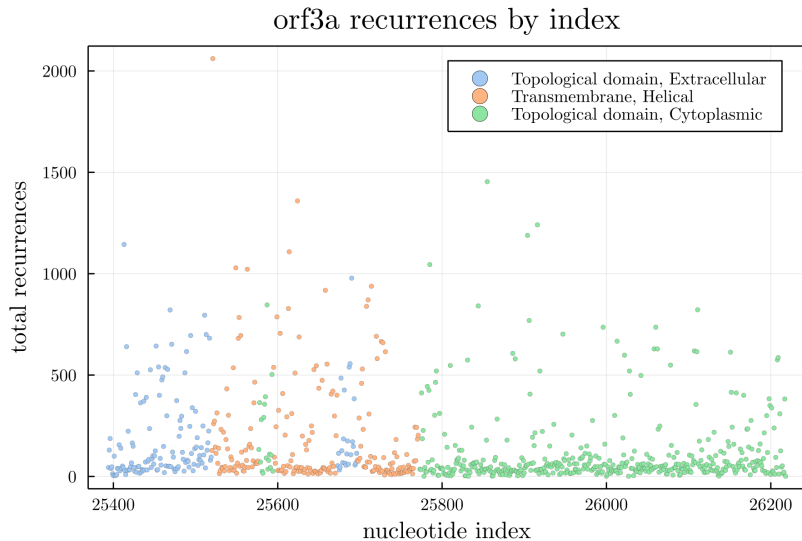
Multidimensional scaling plot using samples from the UK up to mid November

# Homoplasy in global tree



Number of recurrent (homoplastic) mutations per base by gene, (normalized by gene length)

# Homoplasy in orf3a





Bessonov, N., Bocharov, G., Meyerhans, A., Popov, V., and Volpert, V. (2021).

Existence and dynamics of strains in a nonlocal reaction-diffusion model of viral evolution.

*SIAM Journal on Applied Mathematics*, 81(1):107–128.



Gog, J. R. and Grenfell, B. T. (2002).

Dynamics and selection of many-strain pathogens.

*Proceedings of the National Academy of Sciences*, 99(26):17209–17214.



Lapedes, A. and Farber, R. (2001).

The Geometry of Shape Space: Application to Influenza.

*Journal of Theoretical Biology*, 212(1):57–69.



Pedregosa, F., Varoquaux, G., Gramfort, A., Michel, V., Thirion, B., Grisel, O., Blondel, M., Prettenhofer, P., Weiss, R., Dubourg, V., Vanderplas, J., Passos, A., Cournapeau, D., Brucher, M., Perrot, M., and Duchesnay, E. (2011).  
Scikit-learn: Machine learning in Python.  
*Journal of Machine Learning Research*, 12:2825–2830.



Rouzine, I. M. and Rozhnova, G. (2018).  
Antigenic evolution of viruses in host populations.  
*PLoS Pathogens*, 14(9):e1007291.



Smith, D. J., Lapedes, A. S., de Jong, J. C., Bestebroer, T. M., Rimmelzwaan, G. F., Osterhaus, A. D. M. E., and Fouchier, R. A. M. (2004).  
Mapping the Antigenic and Genetic Evolution of Influenza Virus.  
*Science*, 305(5682):371–376.



Starr, T. N., Greaney, A. J., Hilton, S. K., Ellis, D., Crawford, K. H., Dingens, A. S., Navarro, M. J., Bowen, J. E., Tortorici, M. A., Walls, A. C., et al. (2020).

Deep mutational scanning of sars-cov-2 receptor binding domain reveals constraints on folding and ace2 binding. *Cell*, 182(5):1295–1310.



Wilks, S. H., Mühlemann, B., Shen, X., Türeli, S., LeGresley, E. B., Netzl, A., Caniza, M. A., Chacaltana-Huarcaya, J. N., Daniell, X., Datto, M. B., Denny, T. N., Drosten, C., Fouchier, R. A. M., Garcia, P. J., Halfmann, P. J., Jassem, A., Jones, T. C., Kawaoka, Y., Krammer, F., McDanal, C., Pajon, R., Simon, V., Stockwell, M., Tang, H., van Bakel, H., Webby, R., Montefiori, D. C., and Smith, D. J. (2022).

Mapping SARS-CoV-2 antigenic relationships and serological responses.

Preprint, *Immunology*.